Proceedings of the European Conference Physics of Magnetism, Poznań 2017

Magnetic Topological Structures in Multiferroics

Z. Gareeva[a,b,*], K. Zvezdin[c], A. Popkov[d] and A. Zvezdin[c,e]

[a]Institute of Molecule and Crystal Physics, Russia Academy of Sciences, pr. Octyabrya 151, Ufa, Russia

[b]Bashkir State University, ul. Z. Validi, 32, Ufa, Russia

[c]A.M. Prokhorov General Physics Institute, Russia Academy of Sciences, ul.Vavilova 38, Moscow, Russia

[d]National Research University of Electronic Technology, Shokin Square 1, Zelenograd, Moscow, Russia

[e]Faculty of Physics, National Research University Higher School of Economics, Myasnitskaya 20, 101000 Moscow, Russia

In this article we focus on impact of micromagnetic structures on magnetoelectricity of multiferroics. We discuss physical mechanisms of magnetoelectric coupling considering domain walls and spin cycloids. We review the progress on multiferroic materials focusing on high temperature multiferroic: rare earth iron garnet and bismuth ferrite. We argue that topological structures play a pivotal role in multiferoics and show that electric control of magnetism can be carried out via spin spirals and domain walls. Magnetic domain walls produce ferroelectricity in rare earth iron garnets; transformations of spin cycloids release magnetoelectricity in bismuth ferrite. Ferroic orders couple via magnetic inhomogeneities, which shed new light on fundamental physics and applications.

DOI: 10.12693/APhysPolA.133.380

PACS/topics: 75.85.+t, 75.50.Ee, 75.30.Fv, 75.50.Gg,75.60.Ch

1. Introduction

Multiferroic materials fascinate scientists by the exciting opportunities given by coexistence of several ferroic properties whose interaction leads to new physical phenomena and opens wide prospects for technological implementations.

Research on multiferroics starts from the latest 50es when theoretically predicted (Landau, Lifshitz, Dzyaloshinskii) linear magnetoelectric effect was visualized in multiferroic Cr_2O_3 (Astrov, Follen, Rado, Stadler) [1]. The response of the first single–phase multiferroics (bismuth ferrite, manganites, boracites) to magnetic and electric fields stimulated an active scientific research in this area. In the latest 90es the interest to magnetoelectric phenomena has been weakened, however in 2000th a new wave of multiferroics research has been arisen due to the development of technologies allowing synthesize a variety of multiferroic compounds (multiferroic composites and multiphase multiferroics); experimental technique, and quantum computation methods.

New accent of multiferroic research is related to nanoscale objects (domains, domain walls, magnetic vortices) [2]. Uncovering new physical properties such as magnetoelectric pinning, improper (spin driven) ferroelectricity, influence of the strain (strain engineering) on magnetoelectric and cycloidal structures; they bear considerable potential for nanoelectronic devices because of nanoscale dimensions, mobility, controllability etc.

In this article we focus on the high temperature multiferroic bismuth ferrite ($BiFeO_3$ (BFO)) and rare earth iron garnets whose magnetic structures are well established and magnetic topological objects are studied well enough. We analyze the impacts given by inhomogeneous magnetism to ferroelectricity and consider magnetic domain walls and spin cycloids as the tools to manipulate ferroelectric polarization. To reveal this kind of magnetoelectric coupling we explore correlation between structural transformations, ferroelectric and magnetic orders.

2. Incommensurate long periodical spin structures

To exemplify magnetoelectric manipulations via incommensurate cycloid structure we consider the well–known multiferroic $BiFeO_3$ (BFO). BFO has high temperatures of ferroelectric and antiferromagnetic ordering, its crystal structure is a rhombohedrally distorted ABO_3 perovskite with space symmetry group R3c. G–type antiferromagnet ordering is superimposed with long–periodical ($\lambda = 620$ Å) cycloid structure (Fig. 1). Spin cycloid in BFO was experimentally detected during neutron diffraction measurements in 1982 [3], further experiments confirmed the presence of incommensurate cycloid structure; its dependence on the temperature, stresses, doping, action of applied magnetic field has been investigated.

The presence of spin cycloid is consistent with the symmetry of BFO. It was shown in [4] that the energy of inhomogeneous magnetoelectric interaction expressed via Lifshitz invariant

$$\boldsymbol{\Phi}_{me} = \gamma \boldsymbol{P}(\boldsymbol{\mu}\mathrm{div}\boldsymbol{\mu} - (\boldsymbol{\mu}\cdot\mathrm{grad})\,\boldsymbol{\mu}) = \gamma\left(\boldsymbol{P}\left(\boldsymbol{\mu}\mathrm{rot}\boldsymbol{\mu}\right) + \boldsymbol{P}\boldsymbol{\mu}\mathrm{div}\boldsymbol{\mu}\right), \quad (1)$$

where $\boldsymbol{\mu}$ is the magnetic order parameter which in the case of BFO is antiferromagnetic vector $\boldsymbol{L}$, γ is magnetoelectric coefficient ($\gamma \sim 0.6$ erg/cm^3 for BFO), $\boldsymbol{P}$ is the

*corresponding author; e-mail: gzv@anrb.ru

polarization vector ($\boldsymbol{P}\|[111]$ in BFO) stabilizes incommensurate spin modulated structure.

Minimization of the free energy of a system accounting Lifshitz invariant (1) allows determine the spin distribution across cycloid $\sin\theta = \mathrm{sn}\left(\frac{x}{m}\sqrt{\frac{K}{A}}/m, m\right)$ and the cycloid period $\lambda = 4mK(m)\sqrt{\frac{A}{K}}$ via material parameters (γ, magnetic anisotropy (K), exchange stiffness (A) constants).

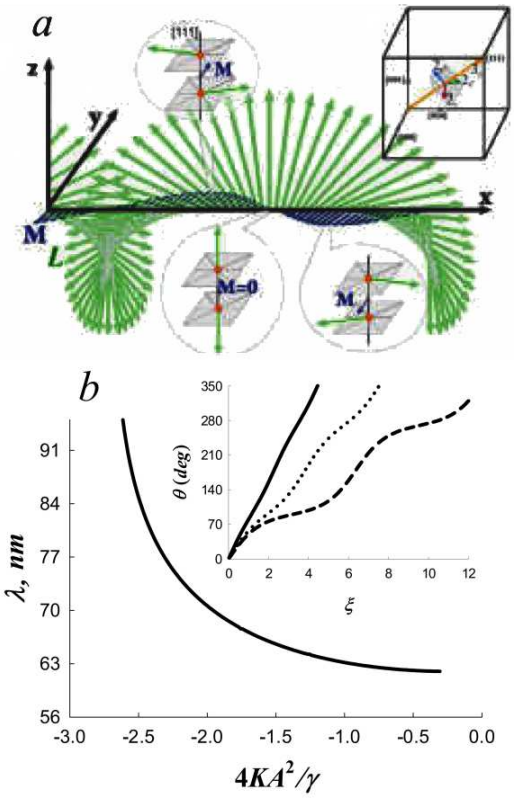

Fig. 1. a) Schematic illustration of spin cycloidal order in BFO (the top right inset shows the orientation of the two- and threefold axes in a cubic perovskite cell), b) dependences of cycloid period λ and angle θ on material parameters.

Cycloidal state hampers linear magnetoelectric effect (LME), allowed by the symmetry of BFO. In order to release LME it is necessary to suppress cycloid. It can be achieved by rare earth ions doping [5], action of high magnetic fields [6, 9]. High magnetic fields induce the transition from cycloidal state into uniform antiferromagnetic phase that is accompanied by essential increase of electric polarization indicating LME (Fig. 2).

Theoretical analysis done in [6, 7, 12] allowed calculate critical field of transition and determine the LME tensor $\hat{\alpha}$ via components of antiferromagnetic vector $\boldsymbol{l} = \boldsymbol{L}/2M_s$.

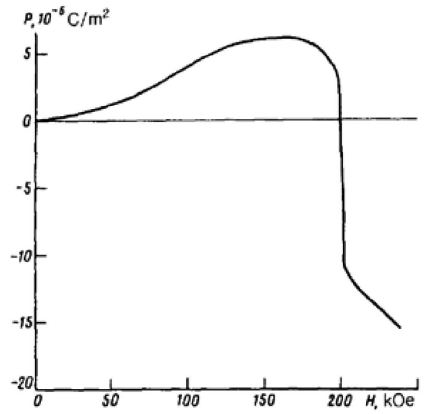

Fig. 2. Longitudinal polarization versus the strength of the magnetic field along the [001] axis at $T = 10$ K [6].

$$\hat{\alpha} = \begin{vmatrix} 0, & a_1 l_z, & -a_2 l_y \\ -a_1 l_z, & 0, & a_2 l_x \\ -a_3 l_y, & a_3 l_x, & 0 \end{vmatrix}. \qquad (2)$$

Strains as the result of epitaxial film growth can also suppress cycloid. The giant magnetoelectric effect was found in BFO films [8]; the measured value of polarization there attains 1 C/m^2.

Currently, the correlation between structural, ferroelectric and magnetic parameters is the subject of active scientific discussions. It was found that structural instabilities including antiphase rotation of oxygen octahedrons significantly affect BFO ferroelectric and magnetic properties [10–15]. In particular, it has been shown in [12] that LME is related to reorientation of antiferrodistortive order parameter (Ω) determining oxygen octahedrons rotation in electric or magnetic field. In terms of parameter $\eta_{ij} = \frac{\partial \Omega_i}{\partial E_j}$, $\boldsymbol{E}$ is external electric field, LME tensor $\hat{\alpha}$ reads

$$\hat{\alpha} = 4\pi \frac{M_s}{\Omega_0} \begin{vmatrix} 0, & \eta_\perp l_z, & -\eta_\perp l_y \\ -\eta_\perp l_z, & 0, & \eta_\perp l_x \\ -\eta_\| l_y, & \eta_\| l_x, & 0 \end{vmatrix}. \qquad (3)$$

The dependence of $\hat{\alpha}$ on electric field calculated in [12] is shown in Fig. 3.

The knowledge of BFO fine structure allows to explain manipulation of magnetic order by electric field [13–15]. Electric field cannot influence directly on magnetic spins, it acts via ferroelectric polarization and antiferrodistortive parameters coupled to magnetic parameter $\boldsymbol{L}$. The structural, ferroelectric and magnetic phase transitions induced by electric field were explained in [13] in frame of extended Landau–Ginsburg approach based on the symmetry and the $\boldsymbol{P} - \boldsymbol{\Omega} - \boldsymbol{L}$ coupling. Another effective method to control spin cycloid is strain engineering. It has been shown in [14, 15] that strain drastically changes cycloidal structure until its destruction. Actually strain can be used for modification of magnetoelectric properties of epitaxial structures in multiferroics (strain engineering).

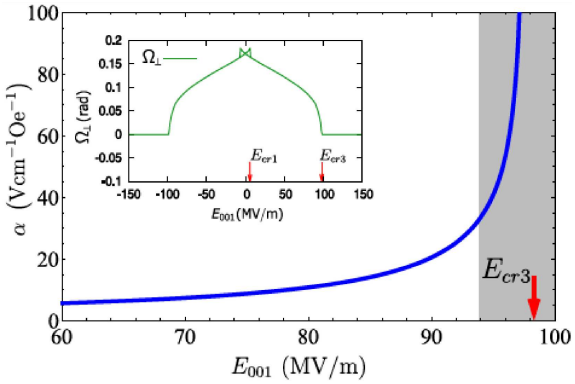

Fig. 3. Dependence of the ME coefficient αon the external electric field applied in [001] direction. (Inset) Dependence of the $\boldsymbol{\Omega}_\perp$ on the applied external electric field [12].

The concept of $\boldsymbol{P}-\boldsymbol{\Omega}-\boldsymbol{L}$ coupling was also attracted to explain interacting magnetic and ferroelectric domain structures [16].

3. Domain walls in multiferroics

Isolated domain walls play an important role in manifestations of magnetoelectricity, being the kind of topological defect, DWs brings its own impact to magnetoelectric coupling of multiferroics. Ferroelectric DWs can serve the pinning centers for antiferromagnetic domain structure [15, 16].

A reverse effect related to magnetic DWs and the other types of inhomogeneous spin distributions also exists: ferroelectricity generated by magnetic ordering is actively discussed. One of the bright examples of DWs tunable ferroelectricity is magnetic DWs in iron garnets, well known magnetic materials with high temperatures of ferromagnetic ordering ($T_c \sim 560$ K). Magnetic DWs in iron garnets produce electric polarization [18–20]; this kind of magnetoelectricity is described by two complementary mechanisms. The first magneteoelectric mechanism is related to the concept of inhomogeneous magnetoelectricity or flexomagnetoelectric effect [17]. Electric polarization is calculated as

$$\boldsymbol{P} = -\frac{\partial \Phi_{me}}{\partial \boldsymbol{E}} = \gamma \chi_e M^2 \left[\boldsymbol{k} \times \boldsymbol{\omega}\right] \qquad (4)$$

where Φ_{me} is the Lifshitz invariant determined by formula (1), M is the magnetization, $\boldsymbol{P}$ is the polarization vector, $\boldsymbol{k}$ is the vector of magnetization inhomogeneity propagation, $\boldsymbol{\omega}$ is the spin rotation axis, $\chi_e h$ is electric susceptibility. Flexomagnetoelectric mechanism allows explain experimentally observed electric response of magnetic DWs to applied voltage [18–20], predict and calculate electric polarization in the vicinity of magnetic DWs of non-Bloch type.

Consider another mechanism of DWs magnetoelectricity related to intrinsic effective field arising due interaction between rare earth (R) and iron (Fe) subsystems. Rare-earth ions in garnet crystals are located in six crystallographically inequivalent positions whose symmetry is described by the D_2 point group that lacks space inversion symmetry operation. Magnetic field produced by Fe sublattice induces the electric–dipole moments of rare-earth ions. In the case of uniform effective field electric dipole moments of rare earth ions constitute antiferroelectric arrangement (Fig. 4).

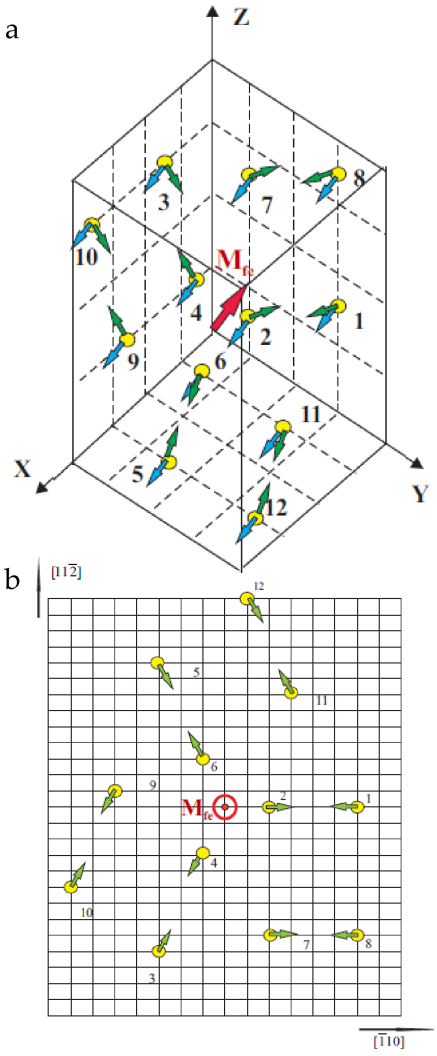

Fig. 4. a) The structure of the magnetic and the electric-dipole moments of Eu^{3+} ion in the primitive cell of $Eu_3Fe_5O_{12}$. The red arrow shows the direction of intrinsic magnetic field related to M_{Fe}. The blue arrows correspond to the magnetic moments of Eu3+ ion and the green arrows correspond to the electric-dipole moments of Eu3+ ion, b) the orientation of the electric dipole moments of Eu^{3+} ion at $M_{\mathrm{Fe}} \| [111]$ [22].

In the case of non–uniform magnetic field antiferroelectric structure becomes broken and electric polarization releases. This mechanism of magnetoelectricity in RIG was discussed in details in [20, 21]. Electric polarization related to electric dipole moments of rare earth ions accompanies magnetic inhomogeneities occurring in RIG including Bloch DWs (Fig. 5) as well as Neel and

twisted DWs. Electric properties of iron garnet films were confirmed by series of experiments on probing of DWs [17–19] by applied voltage. Very recent experimental findings [22] showed that electric field nucleates magnetic bubbles in iron garnet films.

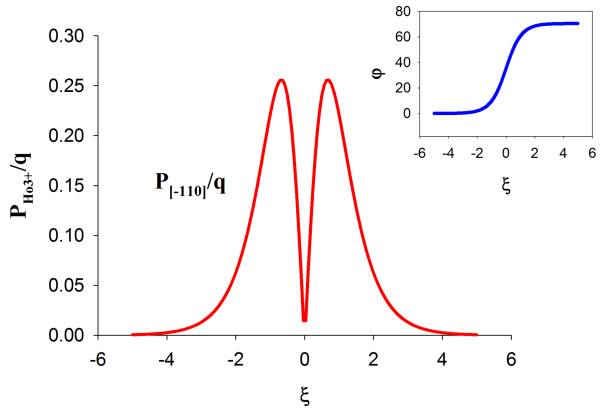

Fig. 5. Distribution of electric polarization at the 180° Bloch DW in HoIG films, $q_{\mathrm{HoIG}(T\sim 4K)} \sim 0.2 \times 10^{-5}$ C/m^2.

4. Conclusions

We consider micromagnetic inhomogeneties in multiferroic materials on example of long range periodical modulated structures and magnetic domain walls. Despite the differences in topologies, dimensions and properties these structures play a pivotal role in manifestation of magnetoelectricity of multiferroics. Magnetoelectric pinning, manipulation of ferroic property by the conjugate field via structural–ferroelectric–magnetic order parameters couplings, phase transformations giving rise to additional magnetoelectricity, magnetic domain walls, bubbles and vortices as the sources of ferroelectricity in magnetic insulators are that small part of topologically induced magnetoelectric effects touched upon in the paper.

We highlighted inhomogeneous structures in high temperature multiferroics bismuth ferrite and rare earth iron garnets, the materials integrated into spintronics. Coupled ferroic orders in conjunction with magnetic inhomogeneities lead to amazing advances in fundamental physics and spintronic technologies; it is perspective for the study of diverse functionalities of multiferroics.

Acknowledgments

The work was supported by the Russian Foundation for Basic Research (grant No. 16-02-00336-A, grant No. 16-29-14037).

References

[1] G.A. Smolenskii, I.E.F. Chupis, *Sov. Phys.-Usp.* **137**, 475 (1982).
[2] G. Catalan, J. Seidel, R. Ramesh, J.F. Scott, *Rev. Mod. Phys.* **84**, 119 (2012).
[3] I. Sosnowska, T.P. Neumaier, E. Steichele, *J. Phys. C: Solid State Physics* **15**, 4835 (1982).
[4] I. Sosnowska, A.K. Zvezdin, *JMMM* **140**, 167 (1995).
[5] Z.V. Gabbasova, et al., *Phys. Lett. A.* **158**, 491 (1991).
[6] Y.F. Popov, et al., *ZhETF Pisma Redaktsiiu* **57**, 69 (1993).
[7] M.M. Tehranchi, N.F. Kubrakov, A.K. Zvezdin, *Ferroelectrics* **204**, 181 (1997).
[8] J. Li, et al., *Appl. Phys. Lett.* **84**, 5261 (2004).
[9] M. Tokunaga, *Frontiers of Physics* **7**, 386 (2012).
[10] C.J. Fennie, *Phys. Rev. Lett.* **100**, 167203 (2008).
[11] A.K. Zvezdin, A.P. Pyatakov, *EuroPhys. Lett.* **99**, 57003 (2012).
[12] A.F. Popkov, et al., *Phys. Rev. B* **93**, 094435 (2016).
[13] A.F. Popkov, et al., *Phys. Rev.B* **92**, 14 (2015).
[14] D. Sando, et al., *Nat. Mater.* **12**, 641 (2013).
[15] A. Agbelele, et al., *Adv. Mater.* **29**, 1602327 (2017).
[16] Z.V. Gareeva, O. Diéguez, J. Íñiguez, A.K. Zvezdin, *physica status solidi (RRL)* **10**, 209 (2015)).
[17] M. Fiebig, D. Meier, *J. Phys.: Cond. Matter* **27**, 463003 (2015).
[18] A.K. Zvezdin, A.P. Pyatakov, *Physics-Uspekhi* **52**, 845 (2009).
[19] A.S. Logginov, et al., *Appl. Phys.Lett.* **93**, 182510 (2008).
[20] N. Khokhlov et al., *Sci. Rep.* **7**, (2017).
[21] A.I. Popov, D.I. Plokhov, A.K. Zvezdin, *Phys. Rev. B* **87**, 024413 (2013).
[22] A.I. Popov, Z.V. Gareeva, A.K. Zvezdin, *Phys. Rev. B* **92**, 144420 (2015).
[23] D.P. Kulikova, et al., *JETP Lett.***104**, 196 (2016).